Nuclear Inst. and Methods in Physics Research, A 887 (2018) 50–53

Contents lists available at ScienceDirect

Nuclear Inst. and Methods in Physics Research, A

journal homepage: www.elsevier.com/locate/nima

Routes for the production of isotopes for PET with high intensity deuteron accelerators

F. Arias de Saavedra *, I. Porras, J. Praena

Departamento de Física Atómica, Molecular y Nuclear Facultad de Ciencias, Universidad de Granada, E-18071, Granada, Spain

ARTICLE INFO

Keywords:
Radioisotopes
PET
Deuterons
Linear accelerator

ABSTRACT

Recent advances in accelerator science are opening new possibilities in different fields of physics. In particular, the development of compact linear accelerators that can provide charged particles of low-medium energy (few MeV) with high current (above mA) allows for the study of new possibilities in neutron production and for new routes for the production of radioisotopes. Keeping in mind how radioisotopes are actually produced in dedicated facilities, we have performed a study of alternative reactions to produce PET isotopes induced by low-energy deuterons. We have fitted the EXFOR cross sections data, used the fitted values of the stopping power by Andersen and Ziegler and calculated by numerical integration the production rate of isotopes for charged particles up to 20 MeV. The results for deuterons up to 3 MeV are compared with the ones from cyclotrons, which are able to provide higher energies to the charged projectiles but with lower intensities. Our results indicate that using linear accelerators may be a good alternative for producing PET isotopes, reducing the problem of neutron activation.

1. Introduction

Positron emission tomography (PET) is becoming an increasingly utilized technique for diagnosis in recent years. PET provides images with better resolution than the most common SPECT technique [1]. The main PET isotopes with their half-lives in minutes are shown in Table 1. The most used of these isotopes is ^{18}F since its half-life of around two hours allows for transportation after production without a dramatic loss of activity. The rest of the isotopes in Table 1 need to be produced in the same place where they are going to be used. ^{11}C is used in ^{11}C-choline to detect the prostate cancer with higher precision than ^{18}FDG [2]. ^{13}N and ^{15}O are used as myocardial perfusion tracers. The first one in $^{13}NH_3$ provides high quality images [3] and the second one, used in $H_2{}^{15}O$, provides also good images after subtracting the blood pool [4].

The standard way of producing the main isotopes used in PET is by accelerating protons in cyclotrons up to energies around 18 MeV with current intensities in the order of a few tens of μA [5]. In the last few years, there has been a lot of interest in the development of a new generation of linear accelerators. These are able to accelerate charged particles to low energies (2–3 MeV) but with mA beam currents. They have advantages compared with cyclotrons used for producing PET isotopes because of their lower operational and construction costs, their reduced requirement for radiation shielding and because they are easier to operate and maintain [6].

The possibility of producing radioisotopes for PET at lower energies lies on the use of deuterons instead of protons, since their coulomb barrier is smaller. This option has been only used extensively in practice for the production of ^{15}O from ^{14}N using cyclotrons accelerating deuterons to 3 MeV, but limits the production yield due to the relatively low current. The possible use of deuterons for the production of ^{18}F and ^{11}C has been proposed by Volkovitsky and Gilliam [7]. In this work, we will study further their pioneering idea and perform precise estimations of the production rate of isotopes for PET, including ^{13}N, by using deuterons from a low energy, high current linear accelerator. Then we will compare these yields to those obtained from protons from a typical higher energy but lower current cyclotron. In Section 2, we describe our method for calculating the production rate. In Section 3, we show our results and finally in Section 4, we present our conclusions.

2. Production rate of isotopes

As we have already mentioned, the main goal of this work is calculating the production rate of isotopes Y for PET, R_Y, in the nuclear reaction $X(x,y)Y$. We have made a more precise estimation of this

* Corresponding author.
E-mail address: arias@ugr.es (F. Arias de Saavedra).

https://doi.org/10.1016/j.nima.2018.01.048
Received 28 July 2017; Received in revised form 9 January 2018; Accepted 15 January 2018
Available online 28 January 2018
0168-9002/

Table 1
Half-life, $T_{1/2}$, of the main isotopes used for PET.

Isotope	^{18}F	^{11}C	^{13}N	^{15}O
$T_{1/2}(min)$	110	20	10	2

quantity than the previous one [7], where the following formula was used:

$$R_Y = \frac{I}{q} n_B \sigma_a R\,, \tag{1}$$

where I is the current intensity of projectiles x that have charge q and initial energy E_i, n_B is the density of nuclei X in the target, σ_a is the average cross section in the range of energies between zero and the initial energy and R is the range of projectile x in the target at E_i.

In order to calculate the production rate of isotopes, we have used the more realistic formula

$$R_Y = \frac{I}{q} n_B \int_{E_i}^{E_f} \frac{\sigma(E)}{\frac{dE}{dx}} dE\,, \tag{2}$$

where we have substituted the averaged cross section and the range of the projectile in the target by integrating on the range of energies from the initial energy E_i to the final one, E_f the ratio of the cross section of the studied reaction and the stopping power of the target on the projectile. As a matter of fact, if we define the stopping power in terms of the thickness of the medium $t = n_B x$ as

$$S_x(E) = \left(-\frac{dE}{dt}\right) = \frac{1}{n_B}\left(-\frac{dE}{dx}\right)\,, \tag{3}$$

we can finally write:

$$R_Y = \frac{I}{q} \int_{E_f}^{E_i} \frac{\sigma(E)}{S_x(E)} dE\,. \tag{4}$$

Once the production rate of isotopes is known, it is easy to calculate the activity of nuclei Y using

$$A_Y(t) = R_Y(1 - e^{-\lambda_Y t})\,, \tag{5}$$

with $\lambda_Y = \ln(2)/T_{1/2}$.

It is obvious that a better description of the process must entail the use of detailed data as a function of the particle energy. In order to perform the numerical calculation of the integral, we must use expressions for both the cross section and the stopping powers that reflect their empirical behavior. We present the expressions that we have used in the following two subsections. The integral in Eq. (4) has been carried out using around two thousand equidistant points in the range of energies and using a compound Newton–Cotes formula with five points [8]

2.1. Parametrizations of cross sections

We have taken the experimental data of the total cross section from the EXFOR database [9]. Since we need to know the cross section for more points than the experimental ones, we have carried out a least-squares fit to the experimental results. Up to provide a good precision in the fit, we have used different functional dependencies. We have fitted for at most four parameters.

Since if we use a linear accelerator we will have a beam with lower energy (3 MeV compared to 18 MeV in cyclotrons), we have to use different nuclear reactions than the standard ones with protons which are endothermic and have a threshold energy of around 2 MeV. We have studied the reactions with deuterons since they are exothermic.

In the case of the reactions ^{20}Ne(d,α)^{18}F and ^{10}B(d,n)^{11}C, we have used a polynomial dependence in order to fit the data of [10] and [11].

$$\sigma(E) = \begin{cases} 0 & E \le c \\ (E-c)(aE+b) & E > c \end{cases}\,. \tag{6}$$

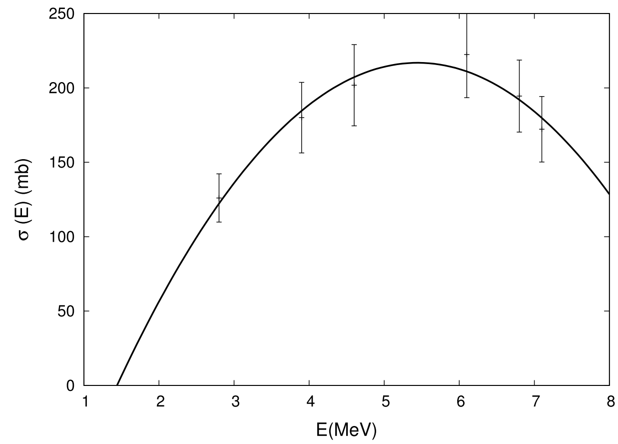

Fig. 1. Parametrization of the cross section of ^{20}Ne(d,α)^{18}F using Eq. (6). The values of the parameters are $a = -13.5$ mb/(MeV)^2, $b = 127.5$ mb/MeV and $c = 1.4$ MeV.

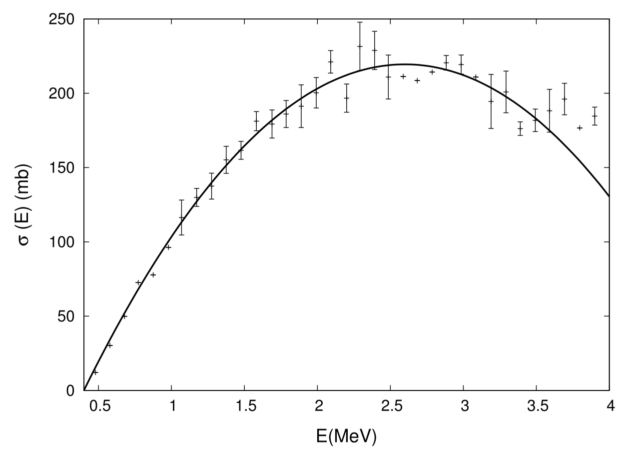

Fig. 2. Parametrization of the cross section of ^{10}B(d,n)^{11}C using Eq. (6). The values of the parameters are $a = -45.36$ mb/(MeV)^2, $b = 218$ mb/MeV and $c = 0.4$ MeV.

We show the results for ^{20}Ne(d,α)^{18}F in Fig. 1 and the ones for ^{10}B(d,n)^{11}C in Fig. 2. The values of the parameters used are given in the corresponding figure caption.

For ^{12}C(d,n)^{13}N we have combined a polynomial and an exponential to fit the data from [12].

$$\sigma(E) = \begin{cases} 0 & E \le b \\ a\dfrac{E-b}{c-b} & b < E \le c \\ ae^{-d(E-c)} & E > c \end{cases}\,. \tag{7}$$

The results are shown in Fig. 3 and the values of the parameters are given in the caption.

For ^{14}N(d,n)^{15}O (data from [13]), ^{18}O(p,n)^{18}F (data from [14]) and the rest of the proton reactions: ^{11}B(p,n)^{11}C (data from [15]), ^{13}C(p,n)^{13}N (data from [12]), and ^{15}N(p,n)^{15}O (data from [16]); we have combined a Gaussian and an exponential dependence for fitting:

$$\sigma(E) = \begin{cases} ae^{-b(E-c)^2} & E \le c \\ ae^{-d(E-c)} & E > c \end{cases}\,. \tag{8}$$

We show the results for ^{14}N(d,n)^{15}O in Fig. 4 and the ones for ^{18}O(p,n)^{18}F in Fig. 5. The values of the parameters used in these reactions and the rest of the proton reactions are given in Table 2.

2.2. Stopping power

In this work, we need data for the stopping power of different media for deuterons and protons. It is known that the main characteristic of